Wavelet Analysis of Hydroclimatic Teleconnections and Precipitation Variability over Ethiopia

Shambel Tsega[1], Getnet Yirga[2], Epherem Minybal[3]

[1,2,3]Department of Physics, Washera Gerospace and Radar Science Laboratory, Bahir Dar University, Bahir Dar, P. O. Box. 79, Ethiopia.

Corresponding author address: getnetyirga41@gmail.com

Abstract

Atmospheric variables like precipitation and stream flow are significantly influenced by various climatic factors and large-scale atmospheric circulation patterns. Investigations into the variation of rainfall by different large-scale oceanic impacts are very fundamental for the economy and climatic maintenance of the country. The study examines the variability of precipitation over Ethiopia through the analysis of monthly and annual rainfall data at five stations in the north, east, west, south, and central parts of Ethiopia from 1987 to 2017 for 31 years. Standardized precipitation ratio (Ip) and wavelet analyses were applied to examine the spatiotemporal variability of precipitation and to determine the effect of oceanic fluctuations on rainfall variability. The calculated standard precipitation index (Ip) indicates the year-to-year variability of rainfall over Ethiopia, which lies between 3.2 and -2. The continuous wavelet technique applied to the yearly time series of precipitations over five stations in Ethiopia reveals short- and long-term periodicities like 2-3, 3-5, and 6–10 years at different time periods. The oceanic indices reveal long-term oscillations like 2-3, 3-5, 6–10, and 8–13 years over different time periods. The rainfall and oceanic fluctuations show similar periodicity in some parts of Ethiopia. Our analysis reveals that the northern part of Ethiopia is negatively affected by Nino-4 during 1992-2003 with a flood event (wet 2.5) around 2001, the southern part is negatively affected by NAO during 2009-2016 with a severe drought (dry -2) in 2014/2015, the western part is negatively affected by SOI during 1992-2005 with two severe droughts observed around 1994/1995 (dry -1.8) and 2003 (dry -2), the eastern part is negatively affected by MOI during 1995-2000 with a drought around 2000/2001, and the central part is negatively affected by Nino-4 during 2002-2010 with a drought (dry -1.3) around 2004/2005.

Keywords: Rainfall: Oceanic Index: Wavelet Analysis: Periodicity: Teleconnection

Introduction

Hydroclimates like precipitation are related to large-scale atmospheric variables via ocean-atmospheric circulations. Such circulation patterns are connected to changes in climatic conditions due to factors like population and technology growth, urbanization and economic development. Variability in precipitation can cause social and economic problems, especially in developing countries like Ethiopia, because their economy is dependent upon the rain-fed agriculture (Singhrattna, 2012). Precipitation variability affects water resources sustainability which includes the availability, management, and utilization of water resources. This, in turn, may affect

ecosystems, land productivity, agriculture, food security, water quantity and human health (Abegaz & Mekoya, 2020). Given its geographical location, the Ethiopian precipitation is significantly influenced by several large-scale atmospheric patterns, such as the El Niño Southern Oscillation (ENSO), the Pacific-North American (PNA) pattern, the North Atlantic Oscillation (NAO), the Pacific Decadal Oscillation (PDO) as well as other teleconnection patterns as reported by different researchers; (Abtew et al., 2009; Diro et al., 2008; Gissila et al., 2004; Korecha & Barnston, 2007; Shanko & Camberlin, 1998).

ENSO has been a subject of intense research over the last three decades, to the extent that SST anomalies in the tropical Pacific are primarily used as main predictors of the Ethiopian rainfall in the forecasting of the National Meteorology Agency (NMA) evaluated the relationships of ENSO indices and the Blue Nile River Basin hydrology. Based on the correlation analysis, high rainfall and high flows are likely to occur during La Nin˜a years and dry years are likely to occur during El Nin˜o years. Extreme dry and wet years are very likely to correspond with ENSO events. The great Ethiopian famine of 1888-1892 corresponds to one of the strongest El Nin˜o years. The IOD had traditionally been viewed as an artifact of the ENSO system although increasingly the evidence is revealing that it is separate and distinct phenomenon. The influence of the IOD is not just confined to the tropical region, but reaching far to the whole globe(Yamagata, 2002). The evidence indicates Indian Ocean SST anomalies have a significant impact on regional atmospheric circulation and rainfall anomalies that extend into East and southern Africa (Marchant et al., 2007).

Better understanding of spatially and temporally organized links between precipitation variability patterns and ocean-atmosphere at large scales would be a considerable asset. Anticipating regional predisposition to rainfall variability in a particular phase of oscillation in the atmosphere–ocean system could help in improving preparedness to emergency (Rathinasamy et al., 2019). The teleconnection between the large-scale oceanic-atmospheric circulation patterns and the variability of precipitation has been a research topic of increasing interest. It is indispensable to study the spatiotemporal characteristics of large-scale climatic factors with the precipitation variability for effective management and allocation of water resources (Das et al., 2020). As a result, this study will focus on the effect of large scale ocean-atmospheric circulation pattern such Niño-4, NAO, SOI, and MOI on the precipitation variability of in different sectors of Ethiopia. The results of this study will help the water resources management agencies of Ethiopia to mitigate the potential impacts of droughts and floods. The variability in hydroclimates encourages engineers, researchers and scientists to work on several related topics aiming at understanding the relationships between local hydroclimates and large-scale atmospheric variables, and at mitigating anomalous events like floods and droughts.

There have been many studies focusing on links of largescale climate anomalies (ENSO) to precipitation variability events in Ethiopia. (Segele et al., 2009) detected the seasonal to inter-annual variability of Ethiopian precipitation and its association with large-scale atmospheric circulation and global Sea Surface temperature (SST). The study has shown that Ethiopian precipitation variability is determined by the combined effects of oscillations of local and regional atmospheric circulation mechanisms and global SST anomaly patterns. In the other studies,(Molla

et al., 2019) also studied the impact of ENSO on precipitation over selected regions of UBNB by applying Pearson correlation analysis.

This study supports that the wavelet approaches, which is very powerful tools to analyze the relationship between multiple time-series in a time-frequency space. In examining the teleconnections, studies have generally used simple regression analysis, and correlation measure (e.g. Pearson's correlation).They have not considered the coherence and interdependency while investigating the teleconnection patterns however some of the large- scale circulation patterns are essentially interdependent (Rathinasamy et al., 2019).

A few studies/no research has been conducted on SOI and MOI which are the prominent climate anomalies that affects precipitation variability of the Ethiopia. In addition to this, the methods they have used provide little in- formation on their inter-relationship and needs further investigation on the time-frequency features of precipitation and climate indices. Thus, this study mainly aims to investigate the teleconnection between precipitation and ENSO, NAO, SOI and MOI over the different sectors using wavelet analysis which leads to estimate the standalone relationship between each climate index and precipitation. In general, we are motivated to study on this area for addressing the problem stated below: How ENSO, NAO, SOI and MOI are linked/teleconnected to the local precipitation variability, which climate anomaly has a significant influence over which local area's precipitation of the Ethiopia. Specifically, the study also identifies the local precipitation (wet and dry) events over the different sectors of Ethiopia by calculating the standard precipitation index (Ip) and explore the periodicity of dominant large-scale ocean indices (ENSO, SOI, NAO, and MOI) that affect the precipitation over the Ethiopia.

Data Source and Method of Analysis

Description of Study Area

Ethiopia is found along 3.30^0N and 15^0N latitude and 33^0E and 48^0 E longitude, with an area of about 1.02 million square km (Korecha & Barnston, 2007). The main natural features of the country consist of a high plateau and mountain chains. Its natural features vary from about 4,500 m above sea level in the north and central region to about 100 m below sea level over the lowland in the northeastern regions of the country. Due to these complex topographical and geographical types, the climate of Ethiopia exhibits strong spatial variations and different rainfall regimes, according to the National Meteorology Service Agency. For instance, the northwestern regions of Ethiopia are described by a single summer (Kiremt) (June_September) rainy season (Tsidu, 2012) with characteristics similar to the Sahel and the Indian monsoon. Kiremt is the main season, occurring from June to September. During this season, the Inter Tropical Convergence Zone (ITCZ), the South Atlantic anticyclone, and the moist southwesterly monsoon flow from the southern hemisphere are the most rain producing structure. The onset and spatial distribution of rainfall also are found to follow the oscillation of the ITCZ and therefore the intensity of the southern hemispheric anticyclones (Segele & Lamb, 2005).The eastern regions exhibit a bimodal (two wet periods throughout the year) pattern long rainy season summer and a second short rainy season in the spring (belg) (February-May); which mainly due to the moist easterly flow from the northwestern Indian Ocean associated with high pressure over the Arabian Sea. Similarly, the southern regions show a bimodal rainfall pattern with maxima in spring and autumn (October-

December), a pattern similar to that found over equatorial eastern Africa caused by the north-south migration of the Intertropical Convergence Zone (ITCZ). The southwestern regions exhibit a unimodal rainfall peak in summer, like the northwest, but they also receive rain- fall throughout the year. The climate mainly varies with altitude, from the hot and arid lowland climate to the cool plateau climate. Lying just north of the Equator, the country experiences little year-round variability in temperature (Zeleke, 2013). Rainfall is caused by the south-western monsoon, which affects the country from June to September (the season is named (Kiremt), but it only affects some regions, namely the highland and mountain slopes exposed to the south-west, while in the south-east of the country there are two rainy seasons, even if less extreme, usually from March to May and October to November (Diro et al., 2011).

Data source

Precipitation data: The main data in this study is daily precipitation from rain gauge for each year and gridded data for the period of 1987-2017 of the selected stations, which are representative of various climatic rainfall zones over Ethiopia provided by the Ethiopian National Meteorology Agency (NMA), Monthly and annual rainfalls data's were derived from the daily data of those stations. Missing data within the time series was filled with data from neighboring years data using interpolation techniques and also, the missing data were filled with gridded data. The gridded data are constructed data series based on records of gauge stations and satellite observations. This gridded data is very helpful due to weather stations are restricted in range and unevenly distributed and have sometimes a short amount of observations. Station selection is based on better available data source. We have used north, south, east, west and central part of the country, which have long range data and representation of various climate zones in the country.

Climate index data: precipitation is teleconnected to several types of climate indices and the knowledge of teleconnections pattern and strength of the interrelationship gives some amount of predictability in remote locations. The data records extracted with in the region of North Atlantic Oscillation (NAO): The NAO is an atmospheric oscillation in sea-level pressure over the North Atlantic Ocean between the Azores subtropical high and the Icelandic polar low. It is calculated as the normalized pressure difference between the Azores and a station in Iceland (50 -200N, 600-300W). Pacific Ocean Nino 4: The strength and sign of the ENSO can be measured by the Nio 4 indices. These monthly indices record the area average SST anomalies in the Nio 4 (5N-5S, 160E-150W) regions, which has SST data set in the time series that ranges from January, 1987-December, 2017 for a period of 31 years. Southern Oscillation Index (SOI): The SOI is another ENSO index, which measures the difference in sea-level atmospheric pressure anomalies between Tahiti and Darwin, Australia(Trenberth, 1984). The negative phase of the SOI occurs when below-normal atmospheric pressure at Tahiti (east-central Pacific) and above-normal pressure at Darwin (west Pacific) are observed. The negative (positive) SOI generally coincide with positive (negative) SST anomalies in the east-central Pacific, associated with an El Nio or La Nina. All climate index data sets are from following website downloaded http://www.esrl.noaa.gov/psd/data/climateindices website.

Methodology

To identify the alternating dry and wet periods of the country in this study the standardized precapitation ratio was first performed on the annual scale. Then, analytical and spectral tools (continuous wavelet Transform analysis) were used to identify the variability modes and determine the origin of this variability.

Standardized Precipitation Ratio (Ip)

The standardized precipitation ratio (Ip) was used to determine wet and dry periods and their alternations consistent with positive (wet) and negative (dry) values(Jemai et al., 2017). It's a dimensionless parameter, based on the ratio of the precipitation difference from the mean to standard deviation (Equation (1). It is defined as follows:

$$I_p = \frac{y_i - \overline{y}}{\sigma} \qquad (1)$$

Where Ip: standardized precipitation ratio, y_i: rainfall for a given study year, $\overline{y}$: average rainfall during a given study period, σ: standard deviation of rainfall for the same period

Wavelet transform

Various methods have been introduced for signal processing and time series analysis. Most of these methods are mathematical transforms that convert vectors or functions from one space to another. Some of the transformations (e.g. Fourier transforms) are only appropriate for the analysis of stationary time series exhibiting a uniform oscillation pattern over time. These transformations are not robust enough for the analysis of non-stationary time series, since they cannot identify all frequencies within the time series(Olkkonen, 2011; Percival & Walden, 2000).

Wavelet analysis is a common method for analyzing the power of local variation within a time series by decomposing a time series into time versus frequency space and hence it describes the variability of precipitation in terms of pattern and representing the contribution of each period/scale for the overall. The wavelet transforms breaking up a signal into scaled versions of a wavelet function; where the size of the wavelet (the window) varies with frequency. The wavelet transform are often used to analyze time series that contain non-stationary power at many various frequencies. Localization during a signal analysis by decomposing or transforming a one-dimensional time Series into a diffuse two-dimensional time-frequency image, at an equivalent time. Then, it is Possible to get information on both the amplitude of any periodic signals within the series, and how this amplitude varies with time. Continuous wavelet transform was chosen because it is widely used complex wavelet having good time-frequency localization than other real wavelets (Addison, 2017).

Wavelet transform is a powerful and accurate mathematical transformation, widely used for signal processing and time series analysis. The theory behind wavelet transform is relatively similar to that of fourier transforms, but offers much greater flexibility allowing a highly accurate capture of all frequencies present in a given time series ((Percival & Walden, 2000; Sang, 2013). Continuous wavelet transform (CWT) is recognized as one of the robust tools for the investigation of processes with high temporal variability ((Labat, 2005). It is appropriate in particular for examining non-stationary processes, like climate variables.

In this study, it is performed on gauge precipitation data and ocean indices to examine their oscillation. The CWT of the signal x(t) generating a wavelet spectrum is expressed as Equation (3.3) (Grossmann and Morlet, 1984).

$$W(s,\tau) = \frac{1}{\sqrt{s}} \int_{-\infty}^{\infty} x(t)\psi^{*} \left(\frac{t-\tau}{s}\right) dt \qquad (2)$$

Every wavelet length is finite and ever precisely localized in time. The mother wavelet includes two parameters: scaling s and temporal location τ

$$\psi_{s,\tau}(t) = \frac{1}{\sqrt{s}} \psi \left(\frac{t-\tau}{s}\right) \qquad (3)$$

With ψs,τ (t): Wavelet daughter; s: scale parameter ; τ : time-localization parameter. and ψ and ψ ∗ represent the wavelet function and complex conjugate, respectively. With τ = 0 and s = 1 denotes the basic or mother wavelet. The flexibility in the wavelet transform comes due to the variations in the scale, which enable to capture the long and short frequency in the time series. Parameterization of scale and wavelet daughters admits the finding of various frequencies that compose signal. The actual computation of the wavelet transform described(Santos et al., 2016). Finally we used mat lab and origin software to analysis the data.

Result and Discussion

Standardized precipitation ratio (Ip)

Precipitation is the result of several atmospheric systems (such as topography and ITCZ) that behave at various scales and periodicity. Further, the irregularity and seasonality exhibited by rainfall, can be assessed by means of the climatic index is crucial. Standardized precipitation ratio(Ip) developed by (McKee et al., 1993) is used to classify the wet and dry rainfall anomalies. Based on the irregularity of precipitation distribution, standardized precipitation was calculated to separate wet and dry periods over 31 years of the study area. For this investigation, we used standardized precipitation ratio equation (1) mentioned in the method of data analysis. The calculated rainfall irregularity (standardized precipitation ratio) was calculated to indicate the estimated year to year variation of inter annual rainfall expressed in terms of standardized precipitation ratio. Negative standardized rainfall indicates dry (below normal rainfall) period and positive anomalies indicate wet (above normal rainfall) period.

Figure 1 depicts the I_p for northern part of the country. Positive standard precipitation values indicate wet periods whereas the negative standard precipitation value shows dry period. For northern part of the study area during the time (1987-1997) was generally dry period with its peak value -1.25 at 1990 and from (1998-2001) wet periods with peak values 2.76 at year 2001. During (2002-2017) more dry period were observed with the occurrence of few slightly humid years. The standard precipitation ratio for this location has shown similar pattern observed by (Ayalew et al., 2012; Wolde-Georgis, 1997). They found positive standardized anomalies in Northern region during 1999-2001.

Figure 2 indicates the standard precipitation ratio of the eastern parts of the county. In the eastern part of the study area from 1987–1991, there was a dry period except in 1987, and the second period (1992–1998) shows generally wet periods with a maximum value of 2.1 around 1996. And the last period (1999–2017) clearly indicates more dry periods compared to wet periods, with a maximum positive peak value (wet) of 2.1 around 2010 and a maximum negative peak value (dry) of -1.5 around 2015.

Figure 4 indicates the standard precipitation ratio for western parts of the country. From the figure, we can observe a slightly dry and wet period during 1987–1996. From 1997 to 2001, wet periods were observed, and the maximum (peak) values of the wet period were observed in 1997 with a value of 2.1. During 2002–2012, we generally observe a dry period with slight humid periods, but in 2003, the negative standard precipitation ratio (dry) reaches a maximum value of -1.8. And from 2013–2017, it shows a wet period with few dry periods.

Figure 3 indicates the standard precipitation ratio for the southern parts of the country. From 1987 to 1994, there were generally dry years with very few wet periods, and from 1995 to 1998, positive values (wet periods) were observed. And from 1999–2005 shows a dry period, and the last period between 2005–2017 was distinguished by an increase in wet years and more frequent dry years compared to the first period or the beginning of the studied period, with a negative peak value reaching -2 in 2015 and a positive peak value of 1.75 at the end of the study period.

Figure 4 indicates the standard precipitation ratio for western parts of the country. As we can see from Figure 5.5, the first period during 1987–1993 shows more wet periods than dry periods, and the second period from 1994–2004 was generally a dry period with a slightly wet period (with a maximum of 3.2 in 1996). The third period (2005–2011) was a wet period except for 2008 and 2009, and the last period (2012–2017) indicates a generally dry period with a maximum negative value of -1.5 in 2014. The positive and negative peak values indicate that there was an extreme event, which led to heavy rainfall and a scarcity of rainfall and water in the country, respectively.

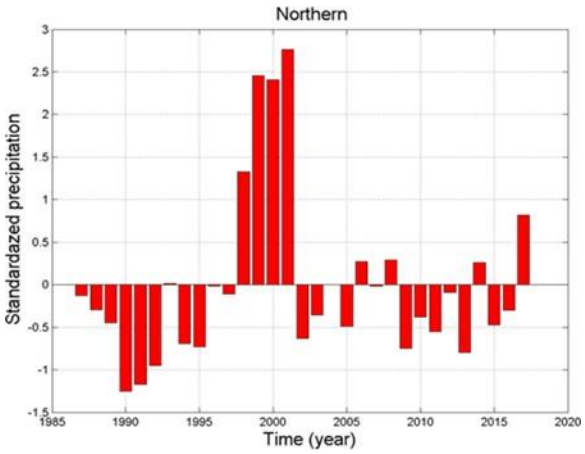

Figure 1 Northern Ethiopia

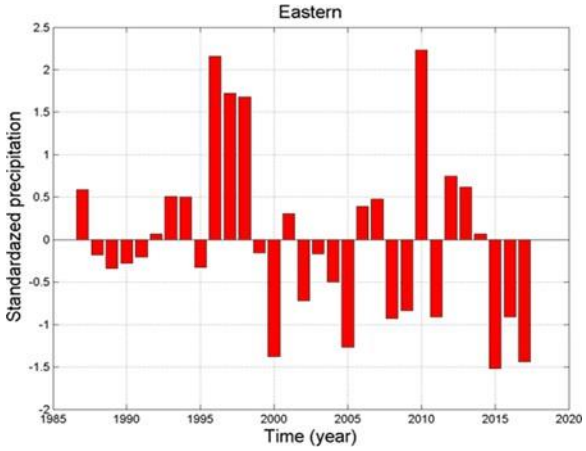

Figure 2 Eastern Ethiopia

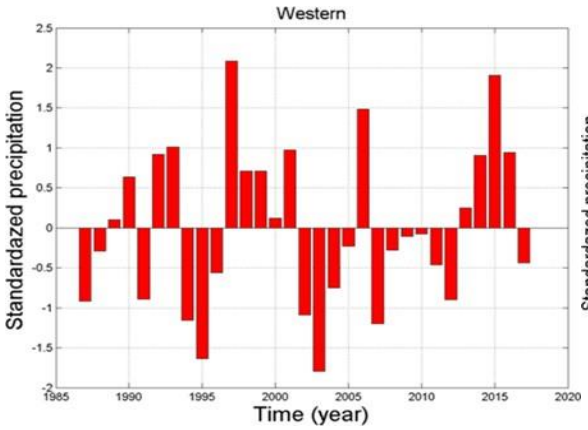

Figure 3 Southern Ethiopia

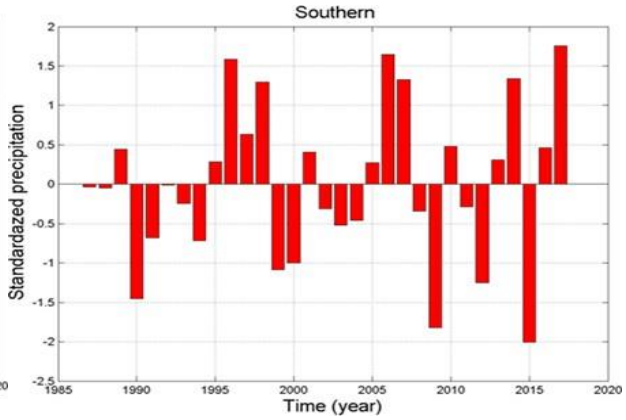

Figure 4 Western Ethiopia

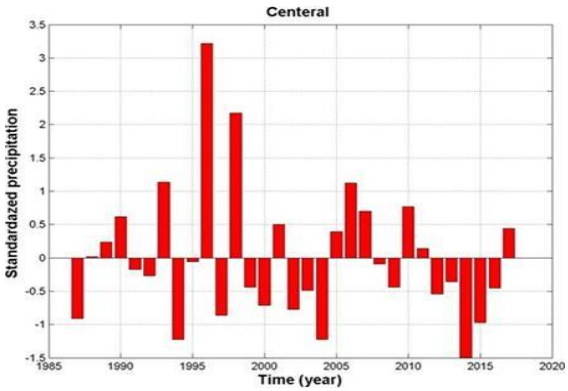

Figure 5 Central Ethiopia

Modes of Rainfall Variability

To understand the precipitation variability and to identify the modes of oscillation, we have applied wavelet transform technique on yearly precipitation data of 31 years (1987-2018) over five selected regions of Ethiopia (Northern, Eastern, Southern, Western and Central) and the results are displayed in figure(6-10). Several frequency modes and powers at annual scales are detected along with dominant periods and their variability in terms of time.

Figure 6 depicts a wavelet analysis of the frequency and time series of rainfall in the northern part of Ethiopia. We can clearly identify the two dominant oscillations, or periodicities. The first oscillation or periodicity of 6–10 years (in terms of frequency 0.1–0.17 with a power of 220 w) prevailed for 11 years from 1992 - 2003.The second oscillation or periodicity was 20 years (frequency of 0.05 with a power of 520 w) during the time from 1992 to 2005. From this, we can determine that the northern part of the country dominates the long-term oscillation of 6–10 years from 1992–2003 and 20 years from 1992–2005. During this period, the standardized precipitation ratio (Figure 1) has shown more wet periods.

Figure 7 describes a wavelet analysis of the frequency and time series of rainfall in the eastern part of Ethiopia. From this graph, we observe three dominant oscillations, or periodicities. The first strong oscillation or periodicity of 2-4 years (frequency of 0.25-0.45 with power of 39 w) prevailed for 4 years from 2008–2012. The second oscillation or periodicity of 5–6.5 years (in terms of frequency 0.15–0.2 with a power of 35 w) lasts from 1995–2000, and the third period periodicity of 10–20 years (frequency of 0.05–0.1 with a power of 110 w) is continued from 1992–2010. So the eastern part of the country dominates the long-term oscillation of 2–4, 5–6.5, and 10–20 years. During the period 1995–2000, standardized precipitation ratios (Ip) show a wet period.

Figure 8 depicts wavelet analysis of frequency verses time series of rainfall for western part of Ethiopia. We can clearly identify the three dominant oscillation or periodicities. The first strong oscillation or periodicity of 3-5 years (in terms of frequency 0.2-0.3 with power of 250w) is prevailed for 13 years from 1992-2005.The second oscillation or periodicity of 8 years (interns of frequency 0.12 with power of 95w) lasts from 1995-2000 and the third period weak periodicity of 27 years (frequency of 0.037 with a power of 20w) is persisted from 1992-1993 years. Therefore we can conclude that western part of the country dominates the long term oscillation of 3-5 for 13 years from 1992-2005. During this time more wet periods were dominates over this region (figure 3).

Figure 9 shows a wavelet analysis of the frequency and time series of rainfall for the southern part of Ethiopia. We can clearly detect two main oscillations, or periodicities. The first strong oscillation or periodicity of 2.5–4 years (in terms of frequency of 0.25–0.4 with a power of 69 w) prevailed for 7 years from 2009–2016. The second oscillation, or periodicity, lasted 10 years (frequency of 0.1 with a power of 97 w) and lasted from 1995 to 2009. Therefore, we can conclude that the southern part of the country dominates the long-term oscillation of 2.5–4 years from 2009–2016 and a 10-year periodicity from 1995–2009. The standard precipitation ratio (Ip) shows a wetter period than a dry period during 1995–2009 over this region (Figure 4).

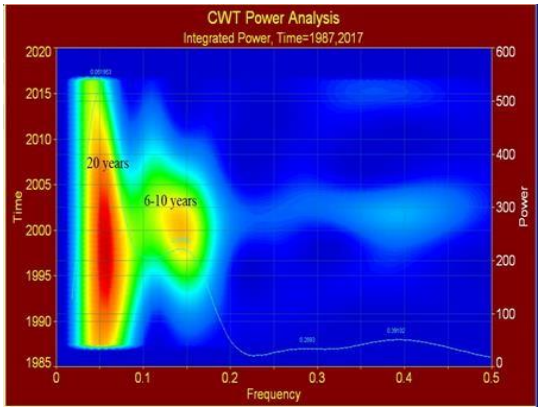

Figure 6 Northern Ethiopia

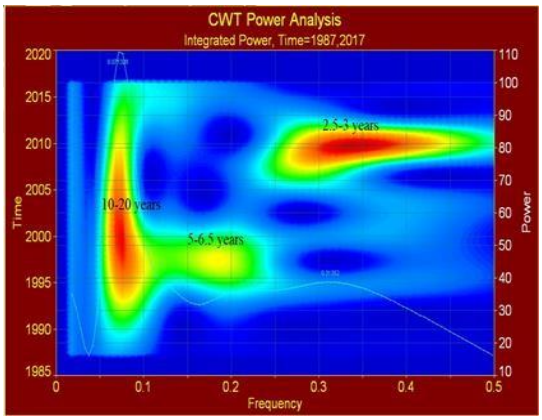

Figure 7 Eastern Ethiopia

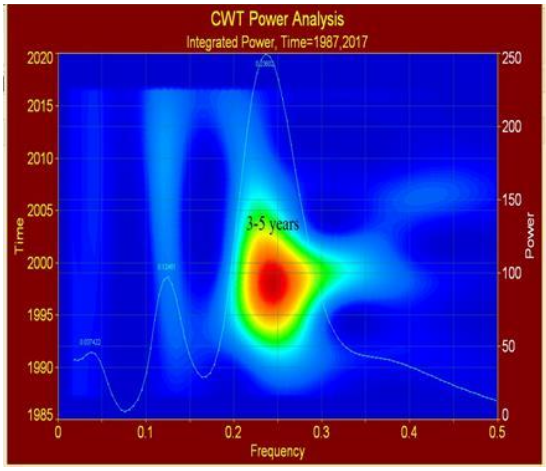

Figure 8 Western Ethiopia

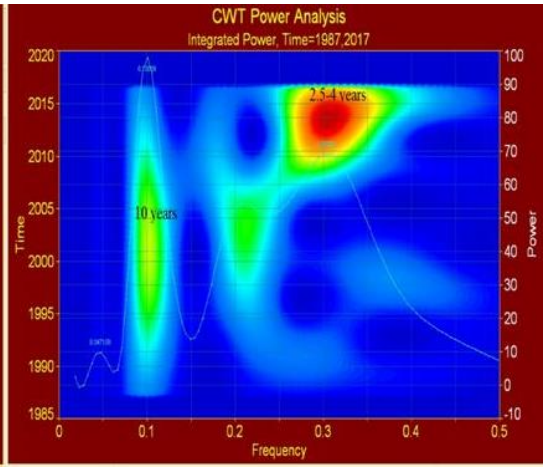

Figure 9 Southern Ethiopia

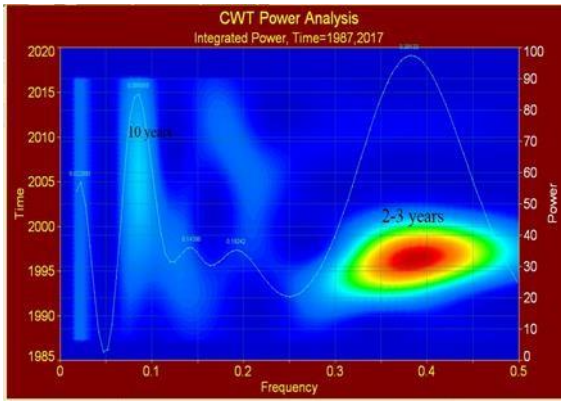

Figure 10 Central Ethiopia

Figure 10 describes a wavelet analysis of the frequency and time series of rainfall in the central part of Ethiopia. We can clearly identify the two dominant oscillations, or periodicities. The first strong oscillation or periodicity of 2-3 years (in terms of frequency 0.35-0.45 with a power of 97 w) prevailed for 8 years from 1992–2000. The second oscillation or periodicity of 10 years (frequency of around 0.1 with a power of 84 w) lasts from 2002–2010. From this observation, we

can conclude that the central part of the country dominates the long-term oscillation of 2-3 from 1992–2000 and the 10-year periodicity of 2002–2010. The standard precipitation ratio (Ip) shows wet and dry periods, but the peak value of the wet period was observed during 1992–2000 with a periodicity of 2–3 years over this region (Figure 5).

Modes of Oceanic Induced Oscillations

To identify the mode of different oceanic index we applied Continuous wavelet transform. Therefore the following contour plot figure (11-14) shows different periodicity of Nino-4, NAO, MOI and SOI oceanic index.

Figure 11 represents the wavelet analysis of frequency verses time series of the Nino-4 index value. From this figure, we can figure out one dominant oscillation. This strong oscillation of 8–13 years (in terms of frequency 0.067–0.125 with a power of 0.32 w) prevailed for 5 years from 1992–2012. This 8–13-year Nino4 oscillation clearly coincides with the periodicities in rainfall data for the north, east, and central parts of Ethiopia. In the northern part of Ethiopia, the observed long-term oscillation of 6–10 years during 1992–2003 clearly coincided with the Nino-4 oscillation from 1992–2012 with a correlation coefficient of -0.84, and during this time period, the standardized precipitation ratio showed more wet periods. The eastern part shows 10–20 year periodicity from 1992–2010 coincided with Nino-4 oscillation with a correlation coefficient of 0.05, and the central part depicts 10 year periodicities from 2002–2010 coincided with Nino-4 oscillation with a correlation of -0.5. Hence, we can conclude that the teleconnection of Nino-4 effects the northern (1992–2003) and central parts (2002–2010) of Ethiopia. Our results are supported by previous studies by (Viste & Sorteberg, 2013; Wolde-Georgis, 1997). They reported that drought was observed during the periods of 1987, 1991, 1994, and 2009 in most parts of Ethiopia.

Figure 12 shows a wavelet analysis of the frequency-versus-time series of NAO oscillation index values. The NAO oceanic index showed two different oscillations, or periodicities. From 2007 to 2012, the first periodicity or oscillation lasted 2-3 years (in terms of frequency of 0.3–0.5 with a power of 0.11 w). The second oscillation, or periodicity, lasted 10–12 years (in terms of frequency 0.083–0.1 and power 0.32) from 1987–1997 and 2007–2015. Among these two oscillations, 2–3 years of NAO oscillation clearly coincide with the periodicities in rainfall data in the southern part of Ethiopia. In the southern part of the country, short-term oscillations of 2.5–4 years (from 2009–2016) clearly coincided with NAO oscillations during the period of 2007–2012 with a correlation coefficient of -0.15, and during this time period, the standardized precipitation ratio showed both wet and dry periods. From this observation, we can conclude that the southern part of rainfall variability relates to the North Atlantic Oscillation Index over 2007–2012. Our result clearly corresponds with the previous study by (Viste & Sorteberg, 2013; Wolde-Georgis, 1997) reported that 1987, 1991, 1994, and 2009 were drought years in Ethiopia.

Figure 13 represents the wavelet analysis of frequency verses time series for MOI index values. The MOI oceanic index depicts one dominant period, which is 6–10 years (frequency of 0.1–0.15 with a power of 0.078 w) from the time 1995-2005.This 6–10 year MOI oscillation clearly coincides with the periodicities in rainfall data for the north, east, and southern parts of Ethiopia. The northern part of the country dominates the long-term oscillation of 6–10 years from 1992–

2003, which clearly coincides with MOI 6–10 year oscillations from 1995–2005 with a correlation of 0.53. During this time, Ip shows wet periods. Eastern part observed 5-6.5 periodicities from 1995–2000 coincides with MOI oscillation of 6–10 years with a correlation of -0.75, and during this time period eastern part Ip shows wetness. The southern part depicts 10-year periodicities from 1995–2009, and the correlation with MOI oscillation is -0.12. Hence, we can conclude that the teleconnection of MOI effects the northern (1992–2003) and eastern parts (1995–2000) of Ethiopia. Moreover, in the northern part during this period (1992–2003).

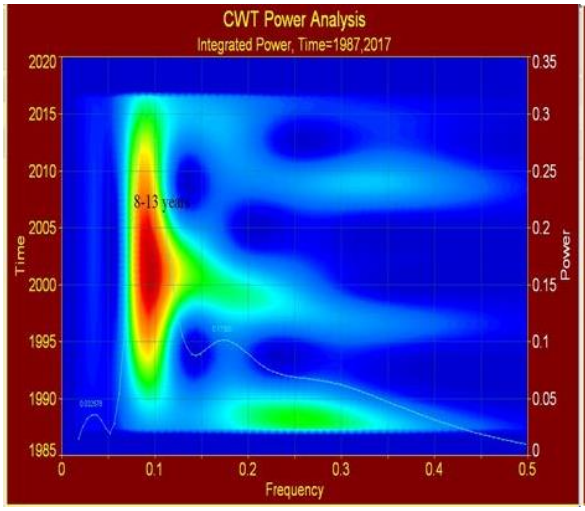

Figure 11 Nino 4 index

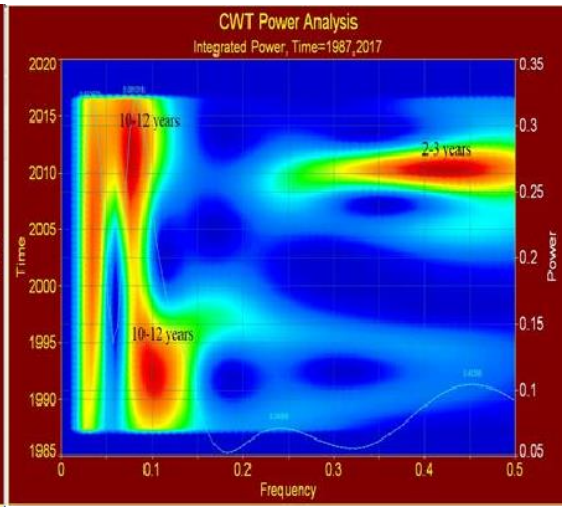

Figure 12 north Atlantic oscillation (NAO)

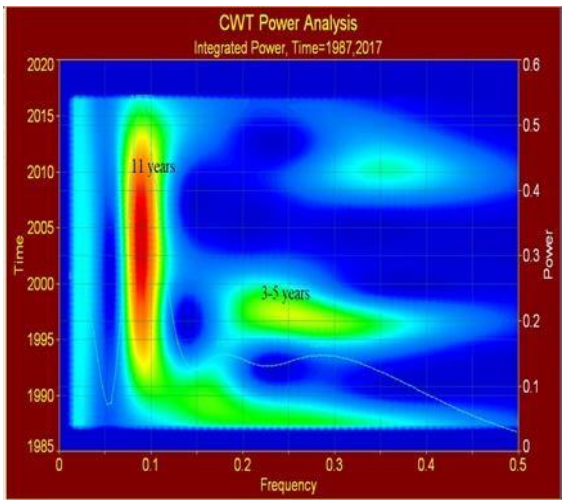

Figure 13 Mediterranean oscillation (MOI) index

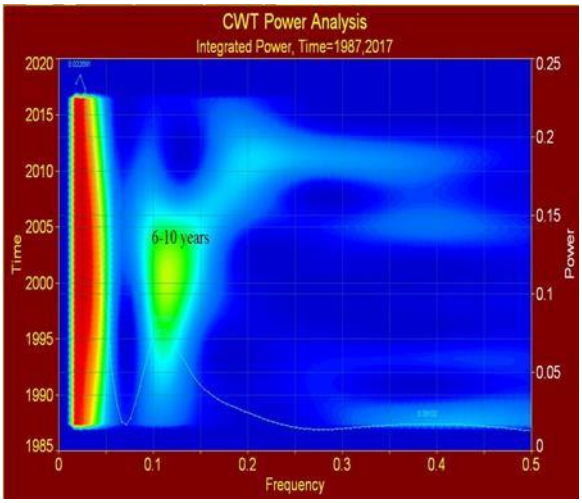

Figure 14 southern oscillation index (SOI)

Figure 14 shows wavelet analysis of frequency verses time series for SOI index values. We can clearly identify the two dominant oscillations, or periodicities. The first strong oscillation or periodicity of 3-5 years (in terms of frequency 0.2–0.3 with a power of 0.15 w) prevailed for 5 years from 1995–2000. The second oscillation, or periodicity, lasted 11 years (frequency of 0.09 with a power of 0.52 w) from 1995-2012.Among these two oscillations, 3-5 years of SOI oscillation clearly coincide with the periodicities in rainfall data in the western part of Ethiopia.

The western part shows a dominant oscillation of 3-5 years from 1992–2005, which coincides with a 3-5 year SOI oscillation with a correlation coefficient of -0.4 from 1995–2000. During this period, the standard precipitation ratio shows a wet period. Hence, we deduce that the southern oscillation index (SOI) affected the western part of Ethiopia during 1992–2005.

Conclusion

This study reveals a dynamic picture of rainfall variability in Ethiopia, characterized by distinct regional patterns and teleconnections with key oceanic indices. Our analysis, spanning 31 years (1987-2017), reveals a significant year-to-year variation in rainfall, with an Inter-annual Precipitation Index (Ip) ranging from 3.2 (wet) to -2 (dry), highlighting the presence of both wet and dry periods within the study period. Wavelet analysis identified distinct periodicities in rainfall for different regions: Northern Ethiopia dominated by 6-10 year and 20-year oscillations; Eastern Ethiopia showing a mix of short and long-term oscillations; Western Ethiopia exhibiting 3-5 year and 13-year periods; Southern Ethiopia with strong 2.5-4 year and 10-year oscillations; and Central Ethiopia marked by 2-3 year and 10-year periodicities. Further analysis reveals strong teleconnections between these rainfall patterns and major oceanic indices, including Nino-4's influence on Northern and Central Ethiopia, the North Atlantic Oscillation's impact on Southern Ethiopia, the Mediterranean Oscillation Index's effect on Northern and Eastern Ethiopia, and the Southern Oscillation Index's influence on Western Ethiopia. Understanding these teleconnections is crucial for predicting future rainfall patterns and developing effective drought mitigation strategies. Further research is needed to explore the socio-economic implications of these patterns and to investigate the influence of other potential climate drivers.

Grant support details

The present research did not receive any financial support.

Conflict of interest

The authors declare that there is not any conflict of interests regarding the publication of this manuscript. In addition, the ethical issues, including plagiarism, informed consent, misconduct, data fabrication and/ or falsification, double publication and/or submission, and redundancy has been completely observed by the authors.

Life science reporting

No life science threat was practiced in this research.

Reference

Abegaz, W. B., & Mekoya, A. (2020). Rainfall variability and trends over Central Ethiopia. *Rema*, *10*(39.58), 2054.

Abtew, W., Melesse, A. M., & Dessalegne, T. (2009). El Niño southern oscillation link to the Blue Nile River basin hydrology. *Hydrological Processes: An International Journal*, *23*(26), 3653-3660.

Addison, P. S. (2017). *The illustrated wavelet transform handbook: introductory theory and applications in science, engineering, medicine and finance*. CRC press.

Ayalew, D., Tesfaye, K., Mamo, G., Yitaferu, B., & Bayu, W. (2012). Variability of rainfall and its current trend in Amhara region, Ethiopia. *African Journal of Agricultural Research*, *7*(10), 1475-1486.

Das, J., Jha, S., & Goyal, M. K. (2020). On the relationship of climatic and monsoon teleconnections with monthly precipitation over meteorologically homogenous regions in India: Wavelet & global coherence approaches. *Atmospheric research*, *238*, 104889.

Diro, G., Grimes, D. I. F., & Black, E. (2011). Teleconnections between Ethiopian summer rainfall and sea surface temperature: part I—observation and modelling. *Climate dynamics*, *37*, 103-119.

Diro, G. T., Black, E., & Grimes, D. (2008). Seasonal forecasting of Ethiopian spring rains. *Meteorological Applications: A journal of forecasting, practical applications, training techniques and modelling*, *15*(1), 73-83.

Gissila, T., Black, E., Grimes, D., & Slingo, J. (2004). Seasonal forecasting of the Ethiopian summer rains. *International Journal of Climatology: A Journal of the Royal Meteorological Society*, *24*(11), 1345-1358.

Jemai, S., Ellouze, M., & Abida, H. (2017). Variability of precipitation in arid climates using the wavelet approach: case study of watershed of Gabes in South-East Tunisia. *Atmosphere*, *8*(9), 178.

Korecha, D., & Barnston, A. G. (2007). Predictability of june–september rainfall in Ethiopia. *Monthly weather review*, *135*(2), 628-650.

Labat, D. (2005). Recent advances in wavelet analyses: Part 1. A review of concepts. *Journal of Hydrology*, *314*(1-4), 275-288.

Marchant, R., Mumbi, C., Behera, S., & Yamagata, T. (2007). The Indian Ocean dipole–the unsung driver of climatic variability in East Africa. *African Journal of Ecology*, *45*(1), 4-16.

McKee, T. B., Doesken, N. J., & Kleist, J. (1993). The relationship of drought frequency and duration to time scales. Proceedings of the 8th Conference on Applied Climatology,

Molla, F., Kebede, A., & Raju, U. J. P. (2019). The impact of the El-Niño southern oscillation precipitation and the surface temperature over the Upper Blue Nile Region. *J. Sci. Res. Rep*, *21*, 1-15.

Olkkonen, H. (2011). *Discrete wavelet transforms: biomedical applications*. BoD–Books on Demand.

Percival, D. B., & Walden, A. T. (2000). *Wavelet methods for time series analysis* (Vol. 4). Cambridge university press.

Rathinasamy, M., Agarwal, A., Sivakumar, B., Marwan, N., & Kurths, J. (2019). Wavelet analysis of precipitation extremes over India and teleconnections to climate indices. *Stochastic Environmental Research and Risk Assessment*, *33*, 2053-2069.

Sang, Y.-F. (2013). A review on the applications of wavelet transform in hydrology time series analysis. *Atmospheric research*, *122*, 8-15.

Santos, C. A., Silva, R. M., & Akrami, S. A. (2016). Rainfall analysis in Klang River basin using continuous wavelet transform. *Journal of Urban and Environmental Engineering*, *10*(1), 3-10.

Segele, Z. T., & Lamb, P. J. (2005). Characterization and variability of Kiremt rainy season over Ethiopia. *Meteorology and Atmospheric Physics*, *89*(1), 153-180.

Segele, Z. T., Lamb, P. J., & Leslie, L. M. (2009). Seasonal-to-interannual variability of Ethiopia/horn of Africa monsoon. Part I: associations of wavelet-filtered large-scale atmospheric circulation and global sea surface temperature. *Journal of Climate*, *22*(12), 3396-3421.

Shanko, D., & Camberlin, P. (1998). The effects of the Southwest Indian Ocean tropical cyclones on Ethiopian drought. *International Journal of Climatology: A Journal of the Royal Meteorological Society*, *18*(12), 1373-1388.

Singhrattna, N. (2012). *Hydrologic forecasting based on statistical and physical approaches for the Upper Chao Phraya River Basin, Thailand* AIT].

Trenberth, K. E. (1984). Signal versus noise in the Southern Oscillation. *Monthly weather review*, *112*(2), 326-332.

Tsidu, G. M. (2012). High-resolution monthly rainfall database for Ethiopia: Homogenization, reconstruction, and gridding. *Journal of Climate*, *25*(24), 8422-8443.

Viste, E. M., & Sorteberg, A. (2013). The effect of moisture transport variability on Ethiopian summer precipitation. *Moisture Transport and Precipitation in Ethiopia*.

Wolde-Georgis, T. (1997). El Nino and drought early warning in Ethiopia. *Internet Journal of African Studies*(2).

Yamagata, T. (2002). The Indian Ocean dipole: A physical entity. *CLIVAR exchanges*, *24*, 15-18, 20-22.

Zeleke, T. (2013). *Assessment of spatial and temporal drought variability and its mechanisms over Ethiopia using observational data analysis and regional climate model experiments* PhD thesis. Addis Ababa University: Addis Ababa].